

INTERMODEL COMPARISON AND EXPERIMENTAL VALIDATION OF ELECTRICAL WATER HEATER MODELS IN TRNSYS

Yannick Allard¹, Michaël Kummert¹, Michel Bernier¹ and Alain Moreau²

¹ École Polytechnique de Montréal, Département de génie mécanique,
P.O. Box 6079, succursale centre-ville, Montréal (Québec) H3C 3A7, Canada

² Laboratoire des Technologies de l'Énergie (LTE), Hydro-Québec,
P.O. Box 990, Shawinigan (Québec) G9N 7N5, Canada

ABSTRACT

This study compares the performance of five electrical water heater models in the TRNSYS environment. The main capabilities, modeling assumptions and performance of the models are first assessed using an intermodel comparison. The main criteria for comparison are: domestic hot water supply temperature, power demand (time-dependent profile and overall energy use) and vertical temperature distribution in the tank. Experimental data are used to validate each model for one specific type of water heater and a selected water draw profile. Finally, the paper makes recommendations for selecting a model and configuring the model parameters in order to minimize the impact of modeling simplifications.

INTRODUCTION

In the province of Québec (Canada), more than 90 % of homes are served by electric water heaters with a total of over 2.7×10^6 units. Domestic water heating makes a significant contribution to the electrical grid peak load and it represents an opportunity for peak shaving. However, load shifting may have some detrimental consequences on the domestic hot water supply temperature if the heating element is deactivated for a long period. Furthermore, a new peak may be caused if a significant number of heaters are reactivated at the same time. Accurate models are required to assess the impact of load management on residential domestic hot water heaters.

The local standard residential electric water heaters consist of a cylindrical tank with typical nominal capacities of 180 L or 270 L. Hot water leaves by the top and cold water enters directly in the bottom or is brought from the top by an internal pipe. Water is heated by two horizontal elements with a rated power ranging from 3 to 4.5 kW. These elements are regulated by two thermostats in a master and slave mode, where the upper element has the priority and the lower element can only be activated if the upper one is off. In practice, the upper and lower heating elements often have the same set point (e.g. 60 °C) but the upper element has a larger deadband (10 °C) than the lower element (5 °C). This results in the lower element being activated most of the time, even though it has a lower priority in theory.

OBJECTIVE

The purpose of this study is to assess the level of modelling detail that is required to obtain acceptable predictions and to select the most appropriate model among the ones available in TRNSYS; in the context of assessing demand-side management scenarios for residential domestic water heaters.

COMPARED MODELS

The storage tank models considered for this study were selected for their ability to represent a typical electrical water heater, i.e. a vertical cylindrical tank with two heating elements. Five TRNSYS models (referred to as "Types") were identified:

- three Types from the standard TRNSYS library: "TYPE 38" (plug flow tank model), "TYPE 4" and "TYPE 60" (two different stratified tank models based on a nodal approach)
- one TYPE from the TESS component libraries: "TYPE 534" (detailed stratified tank using a nodal approach)
- one non-standard component distributed by Transsolar: "TYPE 340" (multi-port water storage using a nodal approach).

It should be noted that "TYPE 38" and "TYPE 340" can only model one heating elements but they were considered in this study – the results below will show that the upper element is never used in the experimental and intermodel comparison tests.

The selected models can be organized in two main categories. They will be referred to the nodal and plug-flow approach. In the nodal approach, the tank is modelled by a fixed number of nodes (control volumes that hold a fixed amount of water at a fixed height in the tank). In the plug-flow approach, the tank nodal segmentation varies during the simulation and is controlled by the simulation time step, leaving and entering flow rates and node temperatures. Both categories of models share most of the same input data: geometry, material properties, etc. They offer a different level of flexibility to model specific options and configurations. Available options for each studied model are presented in Table 1.

Table 1: TRNSYS models characteristics

	NODAL				PLUG FLOW
	TYPE 4	TYPE 60	TYPE 534	TYPE 340	TYPE 38
NODES					
maximum number of nodes	100	100	500	200	(45)
unequal size nodes	✓	✓			✓
INLET MODE					
load flow enters at the bottom	✓				✓
load flow enters at the specify node	✓	✓	✓	✓	
load flow enters at the closest temperature node	✓	✓	✓	✓	✓
load flow is fractioned and enters at specify nodes			✓		
HEATING ELEMENTS					
maximum number of heating elements	2	2	# nodes	1	1
internal temperature control	✓	✓		✓	✓
ENERGY BALANCE					
Flow Streams					
fully mixed before entering each node	✓	✓	✓	✓	(plug flow)
Thermal losses					
constant overall tank loss coefficient	✓	✓			✓
nodes specified loss coefficient	✓	✓	✓		
zones (top, bottom, edges) specified loss coefficient			✓	✓	
Heat diffusivity					
accounts for thermal conductivity (fluid + tank wall)		✓	✓	✓	✓
Temperature inversion (instability)					
fully mix appropriate nodes	✓	✓	✓	✓	✓
use of a mixing flow rate			✓	✓	

EXPERIMENTAL PROCEDURE

Description of the experimental set-up

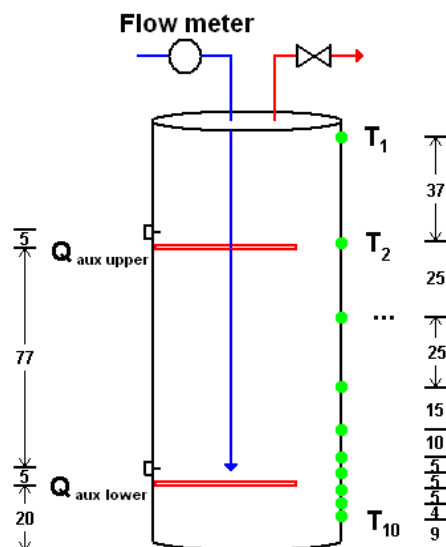


Figure 1 Experimental set-up

Experimentation was made on a commercially available 270 L standard electric water heater storage tank. This glass lined steel tank is commonly used in

residential domestic hot water systems. The electric heater elements are both rated at 4.2 kW. The cold water inlet is at the top of the tank but an internal pipe brings the inlet water to the bottom, approximately at the height of the lower heating element thermostat.

For practical reasons, the vertical temperature distribution has been measured by temperature probes installed on the storage wall, between the steel tank and the insulation layer. Figure 1 shows the location of the temperature measurements (green dots), thermostats and heating elements (the separating distances on the left and right are given in cm). The inlet flow rate is measured by a turbine flow meter and the power used by each heating element is measured independently. A data acquisition system collects data at a 5-min time interval.

The influence of using the tank wall temperature measurement instead of a water temperature measurement inside the tank was investigated numerically in COMSOL (COMSOL Multiphysics 3.5a). The numerical calculations assume a no-flow, pure 1-D conduction problem with a sharp temperature gradient in the tank (thermocline) and typical tank insulation. Results of this analysis are

presented in Figure 2. In regions away from the thermocline, the wall temperature is slightly lower ($\approx 0.1^\circ\text{C}$) than the actual water temperature indicating that there exist a temperature gradient in the tank wall resulting from heat losses to the ambient. Thus, temperature probes underestimate the real water temperature. Furthermore, this effect is amplified at both tank extremities where the contact area with the environment is larger. Near the thermocline, the error introduced by measuring the external wall temperature instead of the water temperature is significant. The affected zone is approximately 3.5 cm in height.

Based on this analysis, a combined measurement uncertainty of $\pm 1^\circ\text{C}$ was assumed for temperature measurements to account for this effect and for thermocouple measurement uncertainty ($\pm 0.5^\circ\text{C}$).

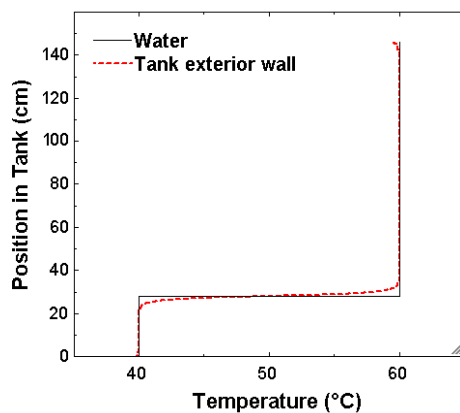


Figure 2 Simulated water and tank temperatures for a 1-D no-flow pure conduction case.

Experimental procedure

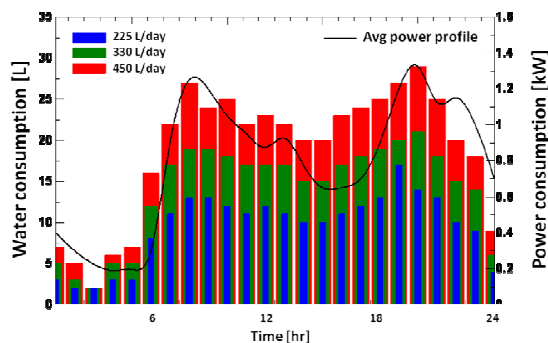


Figure 3 Domestic hot water consumption profiles vs. average diversified demand

Two main tests were carried out:

- standby test: no flow, the tank cools down due to thermal losses to the ambient and is heated by the elements in a steady-periodic regime.
- Normal operation test with different hot water draw profiles (220, 335, 450 L/day). The discharge profile is regulated by a valve that controls the total volume of hot water leaving the tank at a flow rate of 10 L/min. The

different water draw profiles, shown in Figure 3, have been generated in order to approach the average diversified demand of electric water heaters in Québec. These tests include conditions representative of a simple peak management strategy: electric heaters are disabled from 6 AM to 10 AM and 4 PM to 8 PM.

MODEL PARAMETERS

The actual tank geometry was approximated by a cylinder and used in all models. Experimental data were then used to determine the other parameters.

Tank volume segments (nodes)

Based on the relation presented by Kleinbach et al. (1993), the recommended number of nodes can be obtained by:

$$N_{\text{FIXED}} = 45.8 \times T^{-1.218} \quad (1)$$

where T is the number of tank turnover (ratio between the daily water draw and the total tank volume). All nodal models were set to use 58 equal size nodes, which corresponds to the most stringent conditions in this study (average tank turnover = 0.8, i.e. 220 L/day / 270 L).

Inlet mode

For all models that permitted specifying the inlet position, the inlet node was selected to match the position of the end of the internal pipe bringing cold water into the tank. Some models allow to maximize stratification by sending the inlet water volume to the node that is the closest in temperature. This option has not been used here.

Thermostat temperature set point

The set point temperature for the lower heating element $T_{\text{SET_LOW}}$ and the corresponding dead band $\Delta T_{\text{DB_LOW}}$ have been fixed respectively to 56.5°C and 5°C to match the measured behaviour during the standby test (the temperature probe T_7 , near the lower thermostat, was used as a proxy for the thermostat temperature). The values for the upper heating element thermostat could not be estimated from measured data so $T_{\text{SET_UP}}$ was set equal to $T_{\text{SET_LOW}}$ and $\Delta T_{\text{DB_UP}}$ was set at 12.5°C to account for the lowest temperature recorded by the temperature probe T_2 (near the upper thermostat). These parameters correspond to what can be expected for typical water heaters and default manufacturer settings.

Heat loss coefficient

Some models allow modelling specific U-values for each node, but this option was not used in order to keep consistent assumptions between the models.

Two methods were used to calculate the average tank U-value using recorded data from the standby test. The first relies on the steady state heat loss rate ($U_{\text{q_loss}}$), and the second relies on the log-mean

temperature difference (U_{LMTD}), described in (SRCC TM-1, 2008). This U -value is calculated as:

$$U_{LMTD} = \frac{m_{\text{tank}} C_p}{A_{\text{tank}} \text{time}_{\text{decay}}} \ln \left[\frac{(\bar{T}_{\text{tank initial}} - T_{\text{env}})}{(\bar{T}_{\text{tank final}} - T_{\text{env}})} \right] \quad (2)$$

The results of the standby test gave a U_{q_loss} of 1.05 W/m²K, with a measured steady state heat loss rate of 93 W, a total tank surface of 2.6 m², and an average temperature difference ($T_{\text{mean_tank}} - T_{\text{mean_ambient}}$) of 34°C. The value obtained for U_{LMTD} is virtually the same (1.04 W/m²K). The value of 1.05 W/m²K was used in all models.

Studies (e.g. Cruickshank et al., 2010) have shown that assuming an average U -value based on these methods can lead to errors up to 10% in predicting the storage thermal losses. Even if better results can be obtained by calibrating the model with experimental data, the previous U -value results will be considered sufficient in a context where the objective is to obtain a good representation of the entire stock of water heaters.

Heat diffusion rate

De-stratification in the storage tank is mainly driven by thermal conduction within the fluid and conduction along the tank wall. Therefore, the effective conduction k_{eff} in the tank is represented by the sum of k_{fluid} (0.63 W/mK for water) and Δk . This last term may be calculated as (Klein et al., 2010):

$$\Delta k = k_{\text{tank wall}} \frac{A_{\text{c,tank wall}}}{A_{\text{c,water}}} \quad (3)$$

where $k_{\text{tank wall}} = 50$ W/mK corresponding to k_{steel} , $A_{\text{c,tank wall}} = 0.006$ m² is the cross-sectional area of the storage wall and $A_{\text{c,water}} = 0.185$ m² is the cross-sectional area of the water in the tank. This gives $k_{\text{eff}} = 2.25$ W/mK.

Simulation time step

Some models imposed restrictions on the simulation time step. Although this problem is not clearly documented, TYPE 4 will suffer from significant errors in the tank energy balance if the fluid volume of any of the nodes is completely replaced within a given time step (in other words, if the flow rate through a node is equal to or higher than the volume of the node divided by the time step). Given the maximum flow rate in our case is 10 L/min and the node volume of 4.66 L (node has a capacity of 270 L / 58 nodes), the maximum time step is 28 sec. A value of 15 sec was selected for all intermodel tests and for comparison with experimental data.

INTERMODEL COMPARISON

The series of intermodel comparison tests aimed at comparing the ability of different models to calculate the vertical temperature profile in the tank. Two different tests are performed: first, profiles are

compared during and immediately after a water draw event (with all electric heating elements deactivated); then during a charging phase with the bottom electric heating element activated (without any water draw in the tank). To minimize the impact of different initial tank conditions on the results, the last 24 hours of a 72-hour simulation have been analysed. The next sections report the results of these two tests and also present a comparison of CPU calculation times for the different models.

Water draw test

For this test, electric heating elements have been deactivated between 6 AM and 10 AM during the third day of the simulation. At the beginning of each hour, 11 L of water are drawn from the tank with a flow rate of 10 L/min.

Figure 4 shows the temperature in the tank (horizontal axis) versus the height in the tank (vertical axis) at different times of the day (different labelled curves). Results show that the models taking de-stratification into account give similar temperature profiles. TYPE 4 is different since it does not model de-stratification due to thermal conduction, which results in a dead zone in the bottom part of the tank, where the entire lower portion stabilizes at 22°C, which is the ambient temperature. It is also worth noting that the different results for TYPE 60 at the top of the tank are due to numerical errors that only show up in some circumstances. In this particular instance, our tests revealed that the errors would go away if a lower water draw flow rate (e.g. 2 L/h) was used in the simulation. Nevertheless, these results show that TYPE 60 is not as robust as other models tested in this particular case.

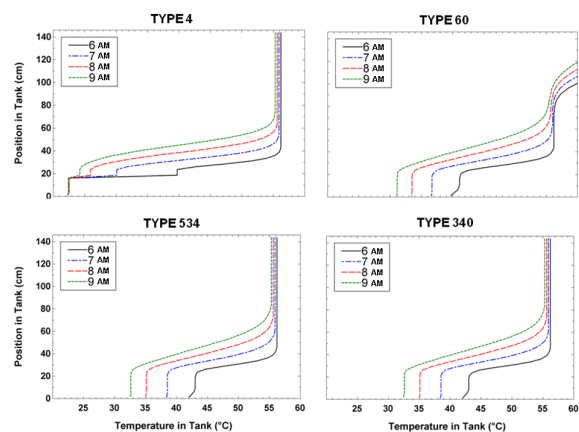


Figure 4 Tank vertical temperature distributions during a water draw

If the cold water inlet is not located at the bottom of the tank, a phenomenon known as temperature inversion can occur during a water draw event. In this case, the temperature at the cold water inlet is lower than the temperature below. This situation cannot physically persist in a real tank and all models have a way to cope with these transient situations. In general, the approach is to completely (and

instantaneously) mix the colder node with the node immediately below (and repeat the process until no inversion remains). Some models (TYPE 534 and 340) allow some control on the speed at which thermal inversion is removed by using a (non-infinite) mixing flow rate between inverted nodes.

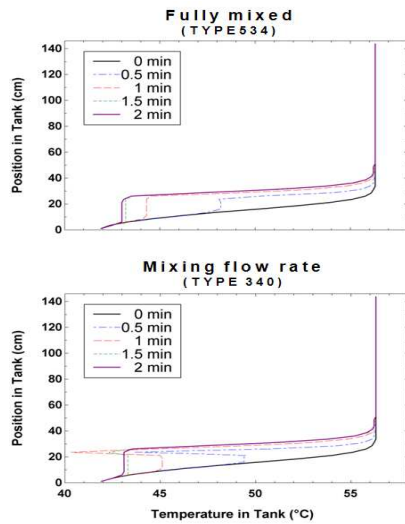


Figure 5 Influence of temperature inversion numerical routine on tank vertical temperature distributions during a single water draw event

The effect of instantaneous mixing and controlled mixing flow rate approaches are compared in Figure 5 for a water draw event. More specifically, TYPE 534 with an instantaneous mixing flow routine and TYPE 340 with default mixing flow rate value have been used during this 1.5 minute withdrawal. The Figure shows that temperature inversion is only significant during the time step when cold water enters the tank. With this relatively small water demand, no difference in the vertical temperature distribution is noticeable after the water draw event.

Electric heaters charging phase

This comparison considered the period just after 10 AM when the electric heater is re-activated after a peak-shaving episode. Again, the last day in a 3-day simulation is used. Simulation results presented in Figure 6 show the evolution of the tank vertical temperature distribution during the charging phase. Similar to the water draw profile test, destratification has an impact on the temperature profile at the bottom of the tank. Part of the heat released by the electric element is transferred by conduction to the lower nodes. As mentioned before, TYPE 4 ignores this effect, which has an impact on the temperature distribution at 10 AM and also introduces a “time-lag” in the profile evolution. TYPE 340 again shows the impact of using a controlled flow rate to suppress temperature inversions in Figure 6 (node containing the heating element is warmer than the nodes above it). This detail has been experimentally validated (Atabaki et al., 2001).

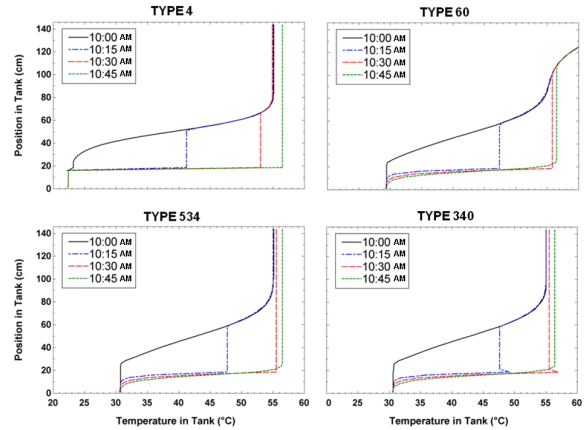


Figure 6 Tank vertical temperature distributions during an electric heater charging phase

Computational efficiency

Table 2 presents the total calculation times for each model, for a 72-h simulation with a 15-sec time step. The results are based on values optionally reported by TRNSYS for each TYPE. In the case of TYPE 534, calculation time for TYPE 1502 (temperature controller) is also accounted for since all other components perform the temperature control inside the TYPE. This contribution is very small (< 2%).

TYPE 38 (Plug-flow) is by far the less computationally intensive, mainly because of the fewer “nodes” (i.e. plugs) of fluid used to model the tank – due to operating conditions, the component typically uses less plugs than the maximum permitted by the model (45) at any given time. All other models use the same number of nodes but they do show significant differences in computational efficiency. TYPE 340 and TYPE 60 are significantly faster. The results also show that the tank turnover T has a significant impact for TYPE 534 on calculation time for a given time step.

Table 2: Calculation time inside TYPES for different number of tank turnover, for a 72-h simulation [sec]

T	TYPE 4	TYPE 60	TYPE 534 +TYPE1502	TYPE 340	TYPE 38
0	21.72	5.79	18.80	4.92	0.35
0.8	20.94	6.40	20.37	4.58	0.31
1.3	22.33	6.42	25.39	4.44	0.35
1.7	22.80	6.53	30.22	3.90	0.36

EXPERIMENTAL VALIDATION

The experimental validation focuses on 3 main performance aspects that could be affected by demand-side management:

- Domestic hot water (DHW) supply temperature (related to user comfort)
- Power demand (time-dependent profile and overall energy use)

- Temperature profile in the tank (e.g. control of bacterial contamination).

Hot water supply temperature

Model predictions for supplied hot water temperature have been compared with the measured data during the last simulation day. As shown in Figure 7, for all models with a nodal approach, except for TYPE 60 (for which numerical errors were encountered), the outlet temperature predicted is within the experimental uncertainty margins ($\pm 1^\circ\text{C}$). The differences can become larger if the heating element is disabled for long periods with a high tank turnover ratio. For the 450 L/day water draw profile, experimental results show a significant temperature drop at the end of the “off” period, which is not reproduced by the models.

The behaviour of the models (represented by the TYPE 534) and the differences with the experimental data are shown in Figure 8 (the green line corresponds to the time of the second dip in Figure 7). The model predicts a step-like transition between a cold zone and a warm zone, while in reality the bottom of the tank is occupied by a slightly warm mixing zone and the top of the tank is not as warm as modelled. The inability of the models to represent the mixing zone accurately will be discussed further below.

The plug-flow model shows a different behaviour and its performance is actually worse for smaller tank turnover ratios (<0.8). The turnover ratio has an impact on the number of “nodes” (plugs) used in the model and it seems that low water draw flow rates result in using a number of plugs that is insufficient to obtain a good accuracy. This is shown in the lower part of Figure 7 for TYPE 38.

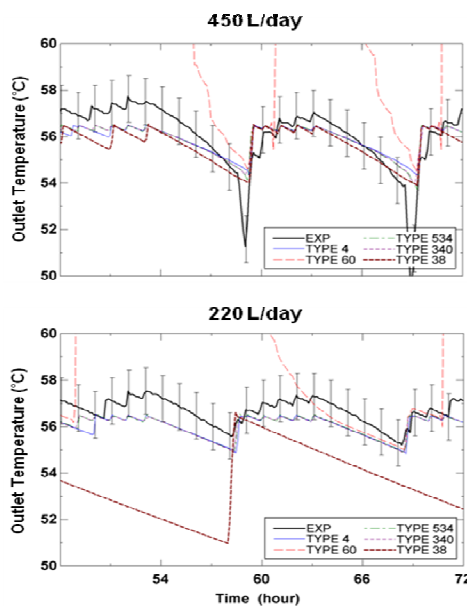


Figure 7 Hot water supply temperature as a function of time for a water draw of 450 and 220 L/day

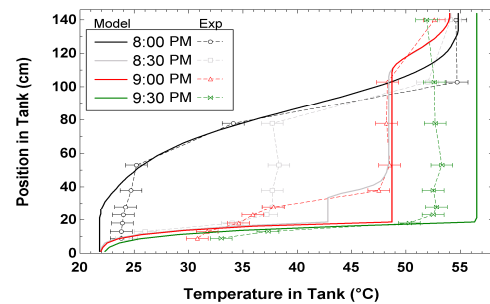


Figure 8: Influence of height and temperature of the mixing zone on the tank supply temperature after a load shifting period for a water draw of 450 L/day

Power demand

Two parameters have been assessed for power demand: the time at which the heating element is operating and the total energy use over 24 hours.

The prediction for the time at which the electrical resistance is activated depends on predicting the thermostat temperature, which is approximated by T_7 in the experimental tests. This temperature is presented in Figure 9, and will be used to evaluate this aspect. Since TYPE 38 does not provide any results on temperatures within the tank, element's power demand Q_{aux} for this model is used instead.

Lower thermostat temperature is mainly influenced by the water draw profile, due to the water inlet position in the tank. For this reason, all nodal models are able to predict the time where the lower element will be activated relatively accurately. For the plug flow model (TYPE 38) some heating events during small water withdraw are missed (model heating period Q_{aux} does not always correspond to experimental lower thermostat temperature increases)

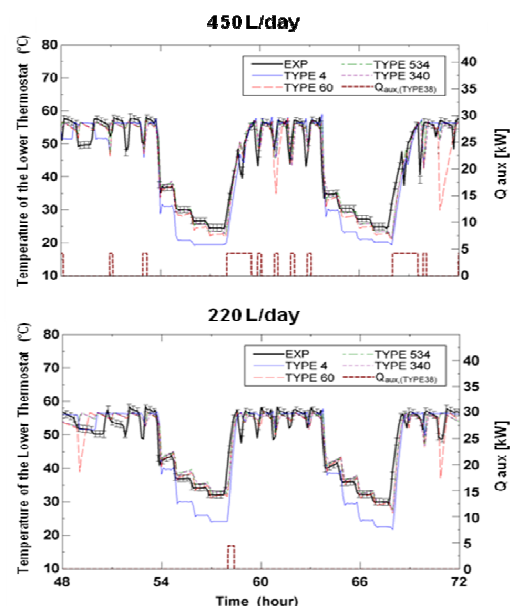


Figure 9 Lower thermostat temperature as a function of time for a water draw of 450 and 220 L/day

This is a limitation of the modelling approach where entering water is supply by the bottom of the tank and large plugs of fluid can be aggregated, reducing the accuracy of the modelled thermostat temperature.

Table 3 presents the total energy use for the last day in a 3-day simulation. The standby test result ($T=0$) only requires electrical heating to compensate for standby losses. The model simplifications for de-stratification (TYPE 4) and nodal segmentation (TYPE 38) result in a larger error. All nodal models with de-stratification underestimate the thermal losses by approximately 10%, which is related to the global tank loss coefficient U_{tank} approximation. This error could have been removed by using a tuned value for the tank global loss coefficient, based on the standby test. For water draw tests ($T>0$), all models give similar results with a small increase ($\approx 6\%$), compared to the standby test, in the underestimation of the overall energy used. Again, TYPE 60 results are affected by numerical errors.

Table 3: 24 h overall energy used in kWh by an electrical water tank as a function of tank turnover

T	EXP	TYPE 4	TYPE 60	TYPE 534	TYPE 340	TYPE 38
0	1.98	1.40	1.77	1.77	1.78	1.38
0.8	12.83	10.57	17.08*	10.76	10.78	10.49
1.3	18.57	15.18	21.96*	15.47	15.47	15.19
1.7	23.83	19.85	26.36*	20.10	20.10	19.83

* Errors occurred at certain time step during simulation.

Temperature distribution

The temperature distribution in the warm zone (upper part of the tank) is mainly constant and dependent on the thermostat set point, T_{SET} , de-stratification modelling and tank heat losses. The sections above show that it is relatively well modelled by the compared TYPES.

Figure 10 shows the temperature profile in the so-called mixing zone region near the cold water inlet position (corresponding to temperature probes T_8 , T_9 and T_{10}). The results show that, under normal operating conditions, models that do not account for thermal conductivity de-stratification (TYPE 4) model a dead-zone, colder than the experimental results. The main advantage of models that do take de-stratification into consideration, is that over time de-stratification effects will correct the temperature distribution in the mixing zone by transferring excess heat from upper nodes (which should be located in the mixing zone) to the nodes located below. In general, models overestimate temperature for nodes located above the heating element (T_8) and underestimate temperature for nodes located under the heating element (T_9 to T_{10}). The vertical temperature distribution obtained for the mixing zone

right after a peak shaving episode should be interpreted with care.

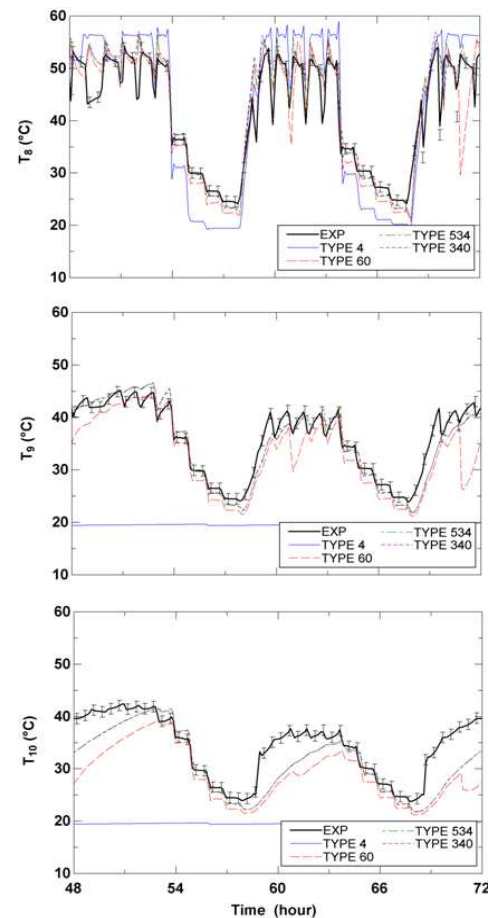


Figure 10 Temperature for different height in the mixing zone vs. time for a water draw of 450 L/day

No model is able to represent correctly the height of the mixing zone. For nodal models, the mixing zone results from removing temperature inversions created in the tank by the entering cold water, which restricts this region below the inlet position. The models can also not represent properly the percentage of heat from the heating element which will be distributed in the mixing zone. For these reasons, the proportion of heat included in the mixing process will be underestimated as shown schematically in Figure 11.

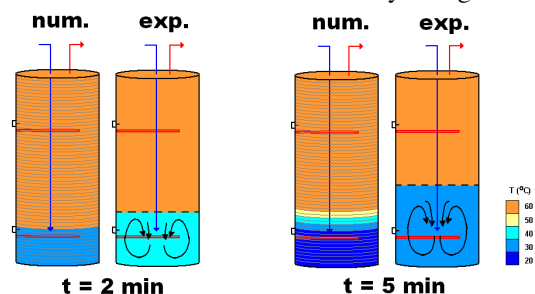


Figure 11 Schematic evolutions in time of the mixing process (comparison between numerical models and experimental measurement)

Mixing zone correction

TYPE 534 offers two options to improve the modelling accuracy in the mixing zone:

- a fractional inlet mode for representing more accurately the entering cold water jet, where the water entering the tank is distributed among different nodes according to user-set fractions.
- using a high number of heating elements to represent the uniform heat distribution throughout the mixing zone during water withdrawal.

Since these fine tuned models have generated better results for a specific water draw profile, it wasn't possible to obtain a general rule that will correctly represent all the water draw profile range.

Result summary

Table 4: Assessment of model accuracy according to key criteria in load management

Criteria	TYPE 4	TYPE 60	TYPE 534	TYPE 340	TYPE 38
Supply temperature	√	X	√	√	O
Energy consumption	O	X	√	√	O
Operation time	√	√	√	√	X
Vertical temperature distribution	X	X	X	X	N/A

√ (Correct)

O (Dependent on water draw profile)

X (Significant difference with measurements)

Table 4 summarizes the results shown above in a qualitative way. TYPE 60 results are affected by significant numerical errors that seem to be dependent on the test being performed. TYPE 534 and TYPE 340 give the best results overall. The vertical temperature profile, especially in the mixing zone, seems to be a weakness in all the tested models.

CONCLUSIONS

Five one-dimensional models of electric water heaters have been investigated and compared to experimental data. The main objective of this study was to assess the usefulness of the different models for demand-side management studies.

The results have shown that for a typical electric hot water heater found in Québec and a typical hot water draw, models based on a nodal approach give a better performance than plug-flow models. The tested plug-flow model (TRNSYS standard TYPE 38) uses a variable number of segments that depends on operating conditions, but this number is never large enough to reproduce the stratification observed experimentally. TYPE 38 is therefore not recommended.

Heat diffusion in the tank has a significant impact on energy performance results, especially for small tank turnover ratios. Therefore, models that do not take in consideration de-stratification (such as TRNSYS standard TYPE 4) are not recommended.

None of the tested models were able to correctly represent the vertical temperature profile in the mixing zone but the models that do consider de-stratification offer a better approximation. TYPE 60 exhibited numerical errors that affected the results significantly in some of the tests and is not recommended. Non-standard TYPE 340 is reasonably accurate and computationally very efficient compared to other nodal models. However, the limitation to one heating element could be a barrier to more general use in modelling typical residential hot water heater in Québec, which have two heating elements. Therefore, TYPE 534 represented the best trade-off amongst the 5 models tested in this paper. It is also the most flexible in terms of number of inlet ports, auxiliary heaters, etc.

REFERENCES

- Atabaki, N. Bernier, M., 2001. Visualisation de la montée d'un panache dans un chauffe-eau électrique, Congrès français de Thermique, SFT 2001, Nantes, 29-31 may 2001
- Cruikshank, C.A., Harrison, S.J., 2010. Heat loss characteristics for a typical solar domestic hot water storage, Energy and Buildings; 42(10):1703-1710.
- Drück, H., 2006, Multiport store – Model for TRNSYS (TYPE 340), Institut für Thermodynamik und Wärmetechnik (ITW), Universität Stuttgart.
- Klein, S.A., et al., 2010, TRNSYS 17 User's manual, Solar Energy Laboratory, University of Wisconsin-Madison.
- Kleinbach, E.M., Beckman, W.A., Klein S.A., 1993. Performance study of one-dimensional model for stratified thermal storage tanks, Solar Energy 50(2):155-166.
- SRCC DOCUMENT TM-1, Solar domestic hot water system and component test protocols, Solar Rating and Certification Corporation 1679 Clearlake Road Cocoa, Florida 32922-5703 (www.solar-rating.org), July 2008.